

Digital mapping of the Mars Pathfinder landing site: Design, acquisition, and derivation of cartographic products for science applications

L. R. Gaddis, R. L. Kirk, J. R. Johnson, L. A. Soderblom, A. W. Ward, J. Barrett, K. Becker, T. Becker, J. Blue, D. Cook, E. Eliason, T. Hare, E. Howington-Kraus, C. Isbell, E. M. Lee, B. Redding, R. Sucharski, and T. Sucharski

Astrogeology Program, U.S. Geological Survey, Flagstaff, Arizona

P. H. Smith and D. T. Britt

Lunar and Planetary Laboratory, University of Arizona, Tucson

Abstract. The Imager for Mars Pathfinder (IMP) acquired more than 16,000 images and provided panoramic views of the surface of Mars at the Mars Pathfinder landing site in Ares Vallis. This paper describes the stereoscopic, multispectral IMP imaging sequences and focuses on their use for digital mapping of the landing site and for deriving cartographic products to support science applications of these data. Two-dimensional cartographic processing of IMP data, as performed via techniques and specialized software developed for ISIS (the U.S. Geological Survey image processing software package), is emphasized. Cartographic processing of IMP data includes ingestion, radiometric correction, establishment of geometric control, coregistration of multiple bands, reprojection, and mosaicking. Photogrammetric processing, an integral part of this cartographic work which utilizes the three-dimensional character of the IMP data, supplements standard processing with geometric control and topographic information [Kirk *et al.*, this issue]. Both cartographic and photogrammetric processing are required for producing seamless image mosaics and for coregistering the multispectral IMP data. Final, controlled IMP cartographic products include spectral cubes, panoramic (360° azimuthal coverage) and planimetric (top view) maps, and topographic data, to be archived on four CD-ROM volumes. Uncontrolled and semicontrolled versions of these products were used to support geologic characterization of the landing site during the nominal and extended missions. Controlled products have allowed determination of the topography of the landing site and environs out to ~60 m, and these data have been used to unravel the history of large- and small-scale geologic processes which shaped the observed landing site. We conclude by summarizing several lessons learned from cartographic processing of IMP data.

1. Introduction

The Mars Pathfinder, or the Sagan Memorial Station, was the first of a series of NASA experiments designed to explore the surface of Mars in the next decade [Golombek, 1997]. The Imager for Mars Pathfinder (IMP), a stereoscopic, multispectral camera, performed a time-critical function in rapidly surveying the surface of Mars to assess the condition of the spacecraft and to assist in deployment of the rover [Smith *et al.*, 1997b; Rover Team, 1997a]. Following these activities, IMP images were acquired in support of several science experiments, including geologic characterization and topographic mapping of the landing site (via acquisition of panoramic and stereo image sequences [Golombek *et al.*,

1997a]), studies of rock composition and mineralogy [Rieder *et al.*, 1997a, b], soil material properties and mineralogy [Rover Team, 1997b], analyses of the wind direction, magnitude, and frequency, atmospheric opacity and water vapor content [Seiff *et al.*, 1997; Schofield *et al.*, 1997], and magnetic properties of wind-blown dust [Hviid *et al.*, 1997]. IMP images provided stunning panoramic views of a variety of rock shapes and textures on a dry, dusty surface of ridges and troughs that probably derived from the actions of water, wind, and impact processes on the landing site in Ares Vallis [Golombek *et al.*, 1997b; Smith *et al.*, 1997a]. This paper describes the design and acquisition of imaging sequences for IMP which have been used to perform digital mapping of the Mars Pathfinder (MPF) landing site and to derive a cartographic product to support ongoing and future science applications of these data. Photogrammetric processing, utilizing the three-dimensional (3-D) character of the IMP data, is a part of our processing effort that is described in more detail in a companion paper by Kirk *et al.* [this issue].

Copyright 1999 by the American Geophysical Union.

Paper number 1998JE900013.
0148-0227/99/1998JE900013\$09.00

Table 1. IMP Geology Filters

Position	Left	Right	Description
0	440	440	"blue stereo"
5	670	670	"red stereo"
6	800	750	
7	860	diopeter lens	
8	900	600	
9	930	530	
10	1000	480	
11	965	965	"IR stereo"

Finally, a summary of lessons learned from cartographic processing of IMP data is presented, with recommendations for design and acquisition of imaging sequences with future landed cameras.

2. IMP Camera and Data Characteristics

The IMP is a stereoscopic imager [Smith *et al.*, 1997b] mounted on an extendable mast which could be deployed to a maximum height of ~1.54 m above the surface (~0.62 m above its stowed location on the lander). IMP operated in both undeployed and deployed states, providing a vertical stereo baseline of ~0.62 m for image acquisition. The IMP camera includes 2 three-element lenses (stopped down to $f/18$ with 23 mm focal length and a $14.0^\circ \times 14.4^\circ$ field of view), two fold mirrors separated by 15 cm for stereo viewing, a 12-element filter wheel (numbered 0 through 11) in each path, and a fold prism placing the images side by side on a single 512×512 pixel CCD focal plane. Each stereo frame has 248×256 active pixel elements (separated by a 12 pixel "dead zone"), with a pixel instantaneous field of view of ~1 mrad (right=0.985 mrad, left=0.981 mrad). The primary stereo-imaging area is from 2 to 10 m from the camera; the toe-in of 37 mrad of the two fold mirrors gives complete overlap of the left and right eye views at a distance of 4 m. Azimuth and elevation motor drives allowed a nearly complete view of the lander, sky, and surface of Mars; the camera pointing range is 360° in azimuth, $+90^\circ$ to -67° in elevation [Smith *et al.*, 1997b].

Of the 24 filters on IMP, 15, with narrow bandpasses centered between 0.4 and 1.1 micrometers (μm), were chosen

and used for geologic studies and stereo viewing of the surface (Table 1) [Smith *et al.*, 1997b]; these filters were selected to be sensitive to iron oxide and pyroxene mineral composition. Of these 15 "geology" filters, six are for acquiring stereo images (at three wavelengths) and nine are in one eye (left or right) only. Stereo pairs were obtained at wavelengths of $0.44 \mu\text{m}$ ("blue"), $0.67 \mu\text{m}$ ("red"), and $0.965 \mu\text{m}$ ("IR"); these are filter positions 0, 5, and 11, respectively. Additional "nongeologic" filters included a magnifying diopeter lens (for viewing magnetic targets on the lander), and left and right eye filters 1 through 4 (used to measure atmospheric water vapor and aerosols). IMP multispectral data are color-balanced using data obtained in situ by the camera from calibration and reference targets mounted on the spacecraft and rover [Reid *et al.*, this issue]. Spacecraft targets include two radiometric calibration targets with shadow posts, geometric targets in the form of fiducial marks on the solar panels, and a five-color target co-mounted with each magnetic and calibration target [Smith *et al.*, 1997b].

3. IMP Imaging Sequences

The IMP camera returned more than 16,000 images, including data for cartography (panoramas) and calibration, spectroscopic analyses of composition, photometric and change detection (multitemporal sequences), and monitoring of rover activities. Here we focus largely on the cartographic imaging sequences. Conservative premission plans to obtain two panoramic data sets from which to map the entire landing site were expanded because the data return rate was higher than expected. A total of five large panoramic imaging sequences, containing over 3500 images, were acquired by IMP during the nominal and extended missions (July 4 through September 27, 1997) at the Sagan Memorial Station landing site in Ares Vallis on Mars (Table 2) [e.g., Kirk *et al.*, 1997, 1998; Soderblom *et al.*, 1997]. Surface operations of the IMP camera following landing included return at the end of the first Martian day (or sol, 24.6 hours) of a lossily compressed, "First Look" or "Mission Success" panorama with partial coverage in color. (A highly compressed panorama taken even earlier to evaluate retraction of the air bags is not listed in Table 2.) On sol 2, late in the day following rover deployment, a full (360°) three-tier, five-filter (including 0L and 0R, or "blue stereo"), "insurance"

Table 2. Panoramic IMP Data Sets for Cartography

Camera Position	Lossy Data Compression	Lossless Data Compression
Undeployed	First Look right camera red (5) $\frac{1}{2}$ azimuth right camera RGB (5,9,0) $<\frac{1}{2}$ azimuth red stereo	Insurance blue stereo right filters 6, 8, 9
Deployed	Monster red stereo $\frac{1}{2}$ elevation right RGB	Super RGB stereo all remaining filters 2:1, near lossless compression "patchwork" of times of day
	Gallery quadrants at four times of day right camera RGB continuous time of day	

RGB, red-green-blue filters.

panorama was obtained and returned with lossless compression, then IMP was deployed on its 0.6-m-high mast. In combination with images taken later in the mission (i.e., from the deployed position), the Insurance Pan provides views of the surface with a large vertical baseline. Beginning on sol 3 and for the following 4 days, IMP operations in the morning included acquisition of a lossily compressed, "Monster" panorama (360° azimuthal coverage with filters 5L and 5R or "red stereo" in all tiers, supplemented by 9R and 0R for "true color" views of the middle two tiers) in support of rover operations and traverse planning. These Monster Pan data have been used to produce widely distributed stereo anaglyphs. The data set can be recognized by the position of the rover at the foot of the rear ramp, near the rock Barnacle Bill [e.g., *Smith et al.*, 1997a, Plate 1b]. On sols 8 to 10, a full three-color (filters 5R, 9R, and 0R but no stereo), lossily compressed "Gallery" panorama was acquired in late morning. The rover is near the rock Yogi [*Smith et al.*, 1997a], and extra images have been added to cover the northern horizon, missing from the Monster Pan because of the tilt ($\sim 3.75^\circ$ to the northeast) of the spacecraft. On sol 13 an intensive photographic survey of the landing site was begun with the goal of returning the highest quality data set possible for multispectral and topographic analyses. The plan was to acquire all 15 filters at each camera position (resulting in multispectral "super cubes"), with three-color stereo pairs at each location, minimal compression, and increased frame-to-frame overlap relative to the earlier pans in order to expedite automatic matching between images and ensure gap-free stereo coverage despite the errors in IMP pointing (accurate to ~ 5 pixels) [*Smith et al.*, 1997b]. The resulting "Super Pan" (Plate 1) was collected over a period of 8 weeks (on sols 13 to 83) at a variety of times of day and, with more than 2000 images, was $\sim 83\%$ complete when contact with the spacecraft was lost. To maximize data quality, red and blue stereo pairs were losslessly compressed (1.3:1), and the remaining 11 frames were compressed 2:1. The vertical and horizontal overlap between frames was increased over earlier mosaics to facilitate automated cartographic processing and stereophotogrammetric reduction. With its inherent multispectral and stereogrammetric capabilities, the Super Pan data set is the ideal focus of topographic and spectroscopic analyses of the MPF landing site [*Soderblom et al.*, 1997; *Gaddis et al.*, 1998; *Kirk et al.*, 1997].

4. Cartographic Processing

4.1. Background

The Super Pan images comprise the most comprehensive cartographic imaging data set acquired by IMP, and they form the basis of all of our cartographic processing. As outlined in this paper, we prepared cartographic products in multiple formats from this data set, supplemented by the other IMP panoramas, using a combination of the U.S. Geological Survey (USGS) Integrated Software for Imagers and Spectrometers (ISIS) and the commercial Digital Photogrammetric Workstation SOftCopy Exploitation Tool (SOCET) Set software from LHZ (Leica/Helava/Zeiss) Systems. ISIS is used predominantly but not exclusively for 2-D "image processing," and SOCET Set is used for 3-D stereophotogrammetric tasks [*Kirk et al.*, this issue]; both

types of processing are required for producing seamless image mosaics and for coregistering the full set of multispectral data. Four primary types of IMP cartographic products have been developed by the USGS: spectral cubes, panoramic maps, planimetric maps, and topographic data (Table 3). In the remainder of this paper, cartographic processing of the IMP data is described in detail, including presentation of the steps required for image processing versus photogrammetric processing. The cartographic products developed for mission support, scientific analysis, and archival phases of the MPF mission are then outlined. A brief summary of some of the current science applications of these data products is presented, followed by a discussion of the implications of the MPF IMP operations for imaging sequence design and processing of cartographic data for future lander missions.

The division of labor between ISIS and SOCET Set software for cartographic processing of IMP data is shown in Figure 1. ISIS is a UNIX-based system developed by the Astrogeology Team of the USGS for performing cartography and scientific analysis of digital data from a variety of planetary missions and imaging instruments [*Batson*, 1990; *Eliason*, 1997; *Gaddis et al.*, 1997; *Torson and Becker*, 1997]. ISIS is in the public domain and is available via the World Wide Web at <http://www.flag.wr.usgs.gov/ISIS>. Relatively rapid development and modification of techniques for radiometric and geometric calibration, and of tools for science analysis of multispectral data (e.g., extraction of spectra, modeling of absorption band depths, and preparation of classified and/or thematic images), are facilitated by the in-house maintenance of ISIS. For IMP cartography, ISIS is used for the image processing steps of data ingestion, calibration, coregistration, simple geometric projection, simple photometric correction, and mosaicking. These steps or "levels" of processing are similar from one instrument to another [*Batson*, 1990; *Eliason*, 1997]. However, because of the unique and complex geometry of the IMP camera, a dedicated ISIS program (IMPJIG) was written to perform bundle adjustment, i.e., simultaneous estimation and improvement of ground-point coordinates and revised camera pointing information for sets of images. The steps required to perform 2-D image processing of IMP data with ISIS are described further below.

SOCET Set (although it incorporates similar functions to ISIS) is used for its unique stereomapping functions: stereoscopic image and graphics display; use of the stereo display and a 3-D input device to perform manual measurement or editing of single points, digital terrain models (DTMs), and geomorphic features; automatic and manual generation of geometric control points and DTMs; contouring, feature extraction, and fully 3-D geometric transformations of points and images such as orthorectification. A small number of new modules were added to this system to ingest ISIS images, to convert ISIS label information on camera pointing and image geometry to that of SOCET Set, to exchange image point measurements with ISIS, and to export DTMs and images to ISIS (including coregistration of the left and right camera images). Use of SOCET set for performing 3-D or stereophotogrammetric processing of IMP data, with emphasis on the complementarity with ISIS, is described briefly below. *Kirk et al.* [this issue] provide more detail.

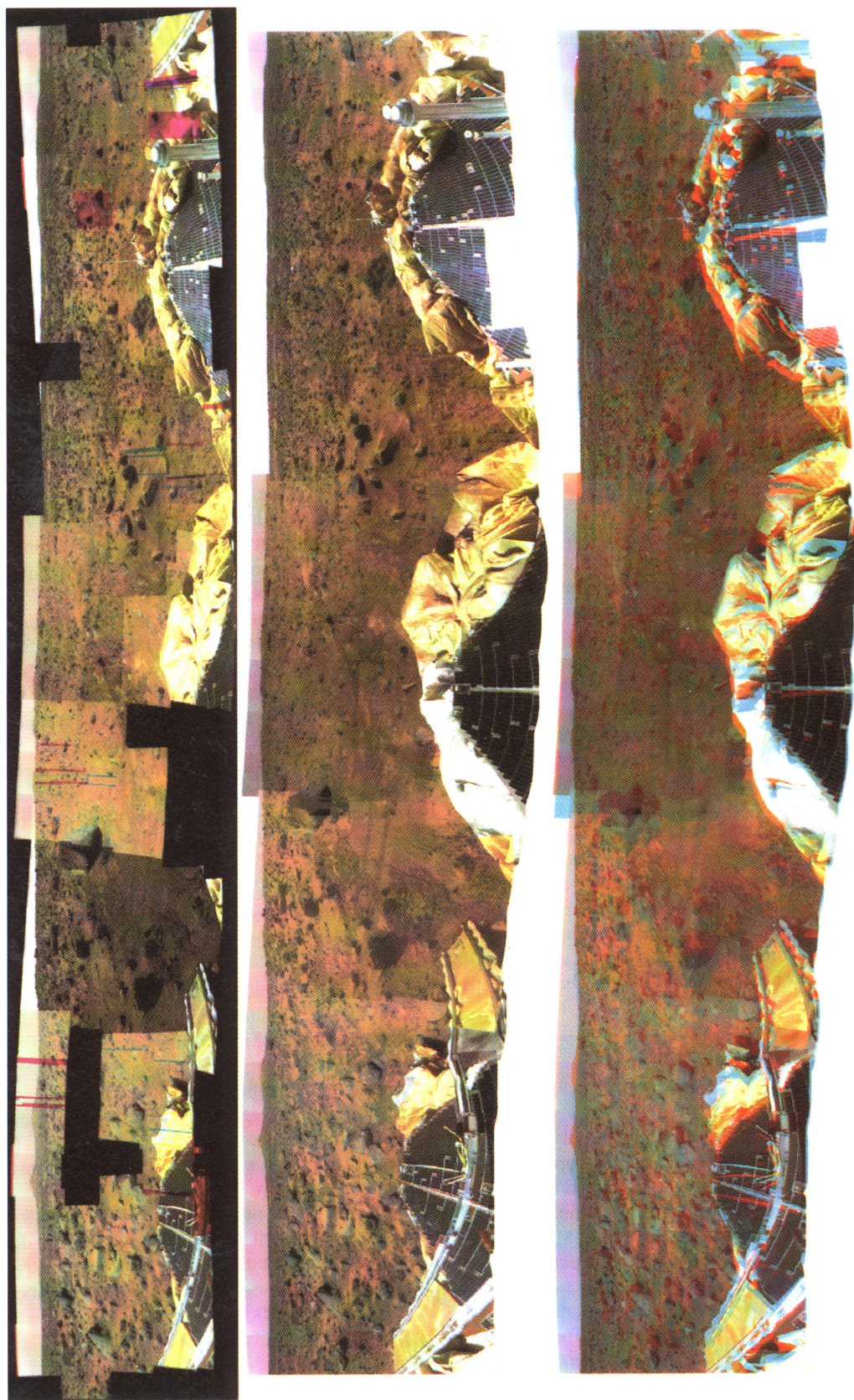


Plate 1. The full Super Pan mosaic contains 119 complete 15-band images or super cubes (1785 images). The interimage brightness variations are due to differing times of day of image acquisition (i.e., lighting was optimized in a given imaging sequence); variation in sky color is due to saturation of data obtained at $0.53\ \mu\text{m}$ ("green") wavelength. (top) A "true color" right eye view of the Super Pan: red= $0.67\ \mu\text{m}$; green= $0.53\ \mu\text{m}$; and blue= $0.44\ \mu\text{m}$. Gaps in the full panoramic coverage represent surface areas which were not imaged at the full 15-band spectral range. Projection is cylindrical; no relative photometric correction has been applied. (middle) Same as top view, but gaps have been filled with data from the Monster Pan. Projection is Macaulay-Kirk. (bottom) Anaglyphic stereo image of the Super Pan: in red is the $0.67\ \mu\text{m}$ mosaic (right eye), and in blue is the $0.44\ \mu\text{m}$ mosaic (left eye). This image may be viewed stereoscopically through glasses with a red filter for the left eye and a blue filter for the right eye. Projection is Macaulay-Kirk. Image resolution is $0.002\ \text{m/pixel}$.

Table 3. Planned USGS IMP Cartographic Data Products

Distribution Format	Point-Perspective Images		Panoramic (Cylindrical) Projection		Cartesian (Overhead) Projection	
	Projected	Rectified	Projected	Rectified	Projected	Rectified
Digital		15-band S-Pan cubes x,y,z, surface normal for cubes	all pans, multiband mosaic for each camera x,y,z coordinates registered to each camera	15-band S-Pan mosaic x,y,z, surface normal		I-Pan color at 1 mm/pixel G-Pan color at 2.8 mm/pixel z at 8 mm/pixel
Hard copy	aligned, aspect corrected vertical stereo pairs (horizon)		all pans, right red filter black-and-white M-Pan anaglyph G-Pan RGB S-Pan false color	black-and-white or color base with contours and nomenclature	1:25 and 1:50 M-Pan color, G-Pan black-and-white (interim)	1:50 color 1:50 with contours, nomenclature <1:50 shaded relief and contours

S-Pan, Super Pan; M-pan, Monster Pan; G-Pan, Gallery Pan; I-Pan, Insurance Pan; RGB, red-green-blue filters.

4.2. Image Processing of IMP data

Cartographic processing of the IMP images with ISIS is a multilevel process that is conducted in several stages (Figure 1), as follows:

1. Level 0 consists of ingestion of raw data records and incorporation of spacecraft, planet, instrument, and camera positional information and navigation data (i.e., SPICE kernels) into ISIS labels.

2. Level 1 consists of radiometric correction involving correction for bad pixels, dark current, shutter effects, flat fields, and conversion of raw pixel values to intensity units ($W/m^2/\mu m/sr$).

3. Level 2 consists of geometric processing, beginning with establishment of geometric control, via interactive selection of relative match points in a single control-base image (i.e., red-filter Super Pan images), addition of hundreds of tie points by SOCET Set, transfer of points to other filters, and calculation and updating of camera-pointing angles by block adjustment. This is followed by subpixel-level coregistration of multiple bands and reprojection to planimetric or panoramic views. Topographic modeling is also part of this step.

4. Level 3 consists of first-order photometric correction, including normalization of scene brightness and removal of residual frame boundaries.

5. Level 4 consists of mosaicking of individual multispectral cubes, possibly followed by cosmetic enhancement or the addition of grids or other annotation.

In Level 0 processing, IMP image data in raw form were imported into ISIS from Experiment Data Record (EDR) files in Planetary Data System (PDS) format from the MPF mission image processing laboratory at the Jet Propulsion Laboratory (JPL). Raw IMP images in EDR format are commonly 2-D, 16-bit images with a header length of less than 256 entries. The ISIS ingestion program (PDS2ISIS) extracts all defined and relevant keywords for later cartographic data processing, including parameters such as a unique image identifier, spacecraft and instrument identification, date and time of observation, exposure time and type, lens and focal plane temperatures, filter number, flags for dark correction, bad

pixels, and shutter effects, and raw azimuth readings and elevation counts (in motor steps). The ISIS file created for raw IMP images is a 3-D "cube" file in 16-bit integer form; the cube is a 2-D image with a band dimension of 1, corresponding to a single filter. IMP2ISIS performs image rotations as necessary (depending on the input data format and whether the image is from the right or left side of the CCD) so that the x dimension of the input file corresponds to the number of lines in the ISIS file, and the y dimension corresponds to the number of samples (the "origin" or (0,0) point of the images is positioned at the upper left).

Level 1 processing includes simple radiometric calibration of IMP images and involves a research effort conducted largely at the University of Arizona [Reid *et al.*, this issue; Crowe *et al.*, 1996]. As implemented in ISIS, radiometric correction steps (developed in close coordination with University of Arizona instrument engineers and incorporating SPICE and other spacecraft ancillary data from JPL) include replacement of bad pixels, subtraction of shutter (zero-exposure) and dark image (fixed exposure, no light) frames to remove the base-level instrument response effects, normalization with a filter- and eye-dependent laboratory flat field file, and (in infrequent cases where no shutter correction was applied on board) correction for readout smear. Corrected pixel values in counts/millisecond are then converted to intensity units of ($W/m^2/\mu m/sr$) using data on the responsivity of the IMP cameras at different temperatures for each eye and filter [Smith *et al.*, 1998b]. The goal of radiometric calibration in ISIS is to enhance the quality of our image products. Further calibration of IMP data to absolute reflectance is an ongoing exercise involving correction for atmospheric effects [Thomas *et al.*, this issue] and verification of reflectance data using the calibration targets at each wavelength [Reid *et al.*, this issue].

Level 2 consists of geometric processing, which includes three tasks: derivation of geometric control, extraction of DTMs, and geometric transformation of the data. Parts of these tasks (picking pass points as inputs for control, and some kinds of geometric reprojection) involve only 2-D image processing techniques, but the majority of Level 2 for

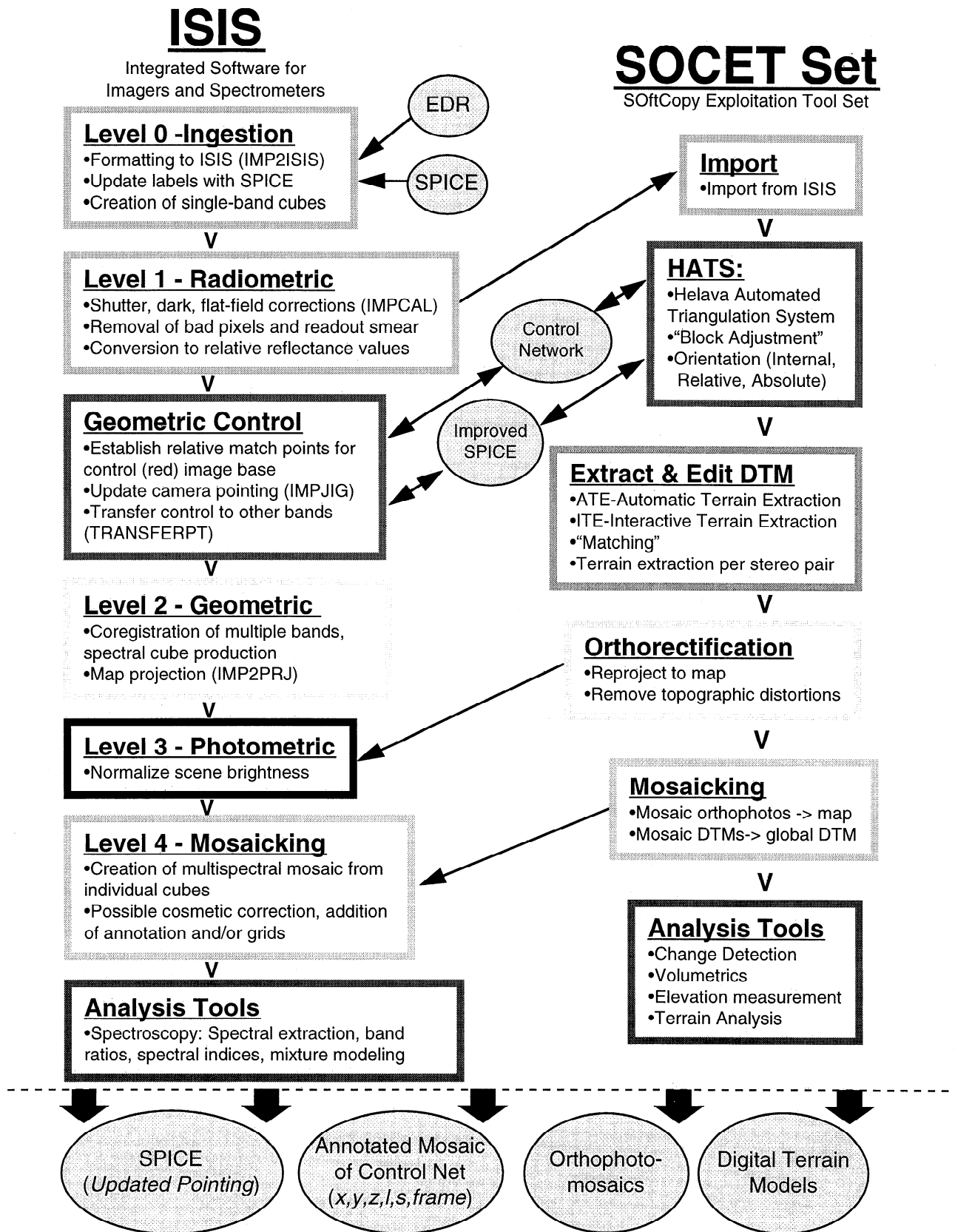


Figure 1. Flow chart of ISIS versus SOCET Set functions in image processing of data from the Imager for Mars Pathfinder (IMP).

IMP data consists of photogrammetric processing [Kirk *et al.*, this issue].

The goal of the geometric control step is to determine the camera-pointing parameters of each image to sufficient accuracy (less than one image pixel) so that accurate geometric measurements can be made and seamless mosaic products can be produced. Products made without refining the camera pointing in this way are referred to as uncontrolled [Batson, 1990]; pointing errors of uncontrolled IMP images are at best ~ 5 pixels [$\sim 0.3^\circ$; Smith *et al.*, 1997b] and commonly as large as 15 pixels ($\sim 1^\circ$). We generated some uncontrolled mosaics early in the mission to support mission operations (e.g., Plate 2). Semiconrolled products are defined as having an ad hoc adjustment to each image in order to reduce mismatches at seams. We produced several semiconrolled mosaics in support of the science analysis phase of the mission. The relative positions of images in these products were adjusted either manually or automatically, based in the latter case on the results of automatic pairwise image matching in the overlap areas (ISIS program RECMOS). All archived products are controlled, meaning that camera pointing for all images was adjusted simultaneously by a rigorous least squares calculation. Because there are no ground control points whose coordinates are known before the mission, pass points can be measured on overlapping images wherever convenient and the ground coordinates of these points must be solved for along with the camera pointing in a process known as bundle adjustment. Our strategy has been to first perform a bundle adjustment of the Super Pan images (which have the best overlap and lowest compression among the imaging sequences) and then to control other data sets by picking pass points between them and the Super Pan. Point measurement was carried out in a combination of manual and automated steps in both ISIS and SOCET Set. An ISIS program, IMPJIG, was written to perform the bundle-adjustment calculation, making use of the known constraints on the IMP such as the dependent pointing of the left and right cameras. Rather than separately bundle-adjust (and then geometrically transform) images taken through various filters of the same camera, we use automatic matching techniques to first calculate relative offsets needed to coregister the images from each camera into a multiband image "cube." These offsets are applied immediately to generate coregistered multiband images. Rather than produce mosaics from the coregistered images, however, we store the calculated offsets and apply them at the same time the data are geometrically reprojected. This approach reduces the number of times the images must be resampled and hence optimizes final image quality.

DTM extraction consists of measurement of a much larger number of points ($\sim 5 \times 10^5$ sitewide, compared to $\sim 10^3$ pass points for control) on stereo pairs and the calculation of their ground coordinates with camera pointing held fixed at the values already determined. Geometric manipulations include both the photogrammetric process of transforming and resampling the data based on the 3-D coordinates of each point in the detailed topographic model, and 2-D image-processing transformations not dependent on the topography. The latter are equivalent to (and mathematically derived as) the 3-D geometric transformations that would be valid if all points on the scene lay on a horizontal ground plane. For convenience, we refer to products that have been transformed

by using the detailed topography as "rectified" and those that have had only a 2-D transformation applied as "projected." We have developed software for transformation to three different coordinate systems, corresponding to the three types of archived image products. In all cases, rectification is performed in SOCET Set, and projection steps are done in ISIS.

4.2.1. Point perspective. This is the original geometry of an image, including the input IMP images. In SOCET Set we used the DTM data derived for a super cube to rectify the 15 images so that they appear as if they were obtained from a single camera located midway between the actual left and right camera positions [Kirk *et al.*, this issue, plates 1a-1c]. The result is a multiband data set coregistered to subpixel accuracy (except for minor residual parallax at the edges of rocks) that is useful for spectroscopic studies. Because these coregistered cubes are geometrically like the original images, they can be further processed by reprojection and mosaicking, for example, into panoramas. Reprojection of images from one camera position to another without point-by-point rectification may also be useful to align predeploy and postdeploy images (i.e., vertical stereo) for more comfortable stereo viewing.

4.2.2. Panoramic. This type of projection yields mosaics that retain the pictorial character of the images with relatively little distortion, yet can show the full, 360° azimuthal extent of the site. Two types of panoramic projection are in use, and it is useful to give the equations that define them here. For both types of panoramas, an image pixel to be transformed is first projected out to a point with Landing Site Cartographic (LSC) coordinates (X, Y, Z). This point may be determined by intersection of the ray corresponding to the pixel with another image ray (for rectified mosaics), or it may be approximated by the intersection of the ray with the datum plane $Z = 0$ (for projected mosaics). Then the location of the pixel in the panorama is determined from the LSC coordinates. The first and simplest type of panorama is called "cylindrical" because it corresponds directly to standard cylindrical polar coordinates (note, however, that azimuth is measured from the Y toward the X axis rather than the reverse). The transformation is

$$\text{Azimuth} = \tan^{-1}\left(\frac{X}{Y}\right), \quad (1a)$$

$$\text{Elevation} = \tan^{-1}\left(\frac{Z - h}{\sqrt{X^2 + Y^2}}\right), \quad (1b)$$

where h is the height of the camera. The inverse transformation, which is useful for producing planimetric maps from panoramic mosaics, is given by

$$X = (Z - h) \frac{\sin(\text{Azimuth})}{\tan(\text{Elevation})}, \quad (1c)$$

$$Y = (Z - h) \frac{\cos(\text{Azimuth})}{\tan(\text{Elevation})}, \quad (1d)$$

Line and sample coordinates in the mosaic correspond to the elevation and azimuth, respectively. Panoramas from the Viking landers were presented in this form; we use it for mosaics of Super Pan data that have been rectified to a single effective camera position at the gimbal center. The second

type of projection was developed independently at the USGS and at JPL [LaVoie *et al.*, this issue] for portrayal of stereo data in panoramic form; projecting unrectified stereo data to simple azimuth-elevation coordinates results in a peculiar and generally undesirable appearance because the recession of the surface toward the horizon is removed, turning the scene into a vertical "wall" on which true topographic highs appear slightly closer than lows [e.g., Smith *et al.*, 1997a, Plate 1b]. In this Macauley-Kirk projection, columns correspond not to radial planes through the gimbal center (i.e., constant feature azimuth) but planes tangent to the circle swept out by the right or left IMP camera (actually, not quite tangent but toed-in by the same small angle as the camera, yielding loci of constant camera-head-pointing azimuth). The transformation used is

$$\text{Azimuth} = \tan^{-1}\left(\frac{X}{Y}\right) \pm \sin^{-1}\left(\frac{\frac{b}{2} - t \sin \gamma}{\sqrt{X^2 + Y^2}}\right), \quad (2a)$$

$$\text{Elevation} = \tan^{-1}\left(\frac{Z-h}{t}\right), \quad (2b)$$

where

$$t = \frac{b}{2} \sin \gamma + \sqrt{X^2 + Y^2 - \left(\frac{b}{2}\right)^2 \cos^2 \gamma},$$

γ is the toe-in angle (taken as positive inward), b is the camera separation, and the top sign refers to the left camera. The inverse of this transformation is

$$X = (Z-h) \frac{\sin(\text{Azimuth} \pm \gamma)}{\tan(\text{Elevation})} \mp \frac{b}{2} \cos(\text{Azimuth}), \quad (2c)$$

$$Y = (Z-h) \frac{\cos(\text{Azimuth} \pm \gamma)}{\tan(\text{Elevation})} \pm \frac{b}{2} \sin(\text{Azimuth}). \quad (2d)$$

To further enhance the realism of stereo viewing of the panoramas, we also adopted a vertical coordinate that is linear in the tangent of elevation rather than elevation itself. Each column of the panorama is thus (locally) equivalent to a point-perspective image and shows an undistorted slice of the landing site when viewed from an appropriate eye point.

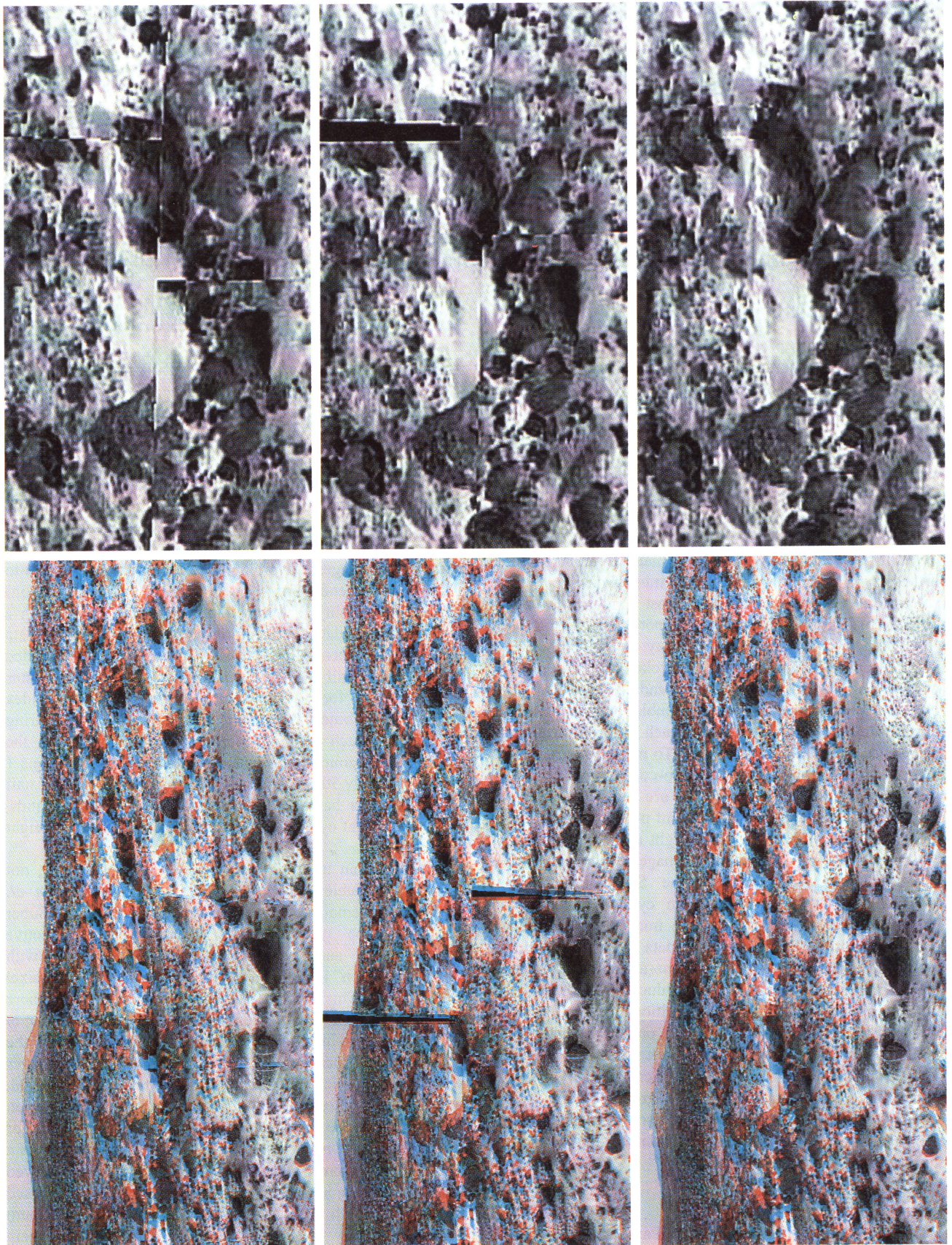
4.2.3. Planimetric. Planimetric products are "maps" of the landing site in a conventional sense, showing a "top view" of features as they would appear projected onto the horizontal (X,Y) plane of a Cartesian coordinate system. Projected planimetric maps were produced in the operations and data-analysis phases of the mission; relief features appear distorted (displaced radially away from the lander) in this format because the projection is accurate only for the mean plane. Archived planimetric maps are rectified; relief features (e.g., rocks) appear in their correct horizontal positions, though gaps in the data set are present in the invisible areas behind such features [Stoker *et al.*, 1997, this issue]. The Cartesian

coordinate system used for our planimetric products is referred to as Landing Site Cartographic (LSC) and differs from coordinate systems used in mission operations. The LSC coordinates are ground-fixed and level, with the positive X direction east, Y north, and Z upward. The origin is chosen at approximate ground level, under the center of the camera gimbal in its initial deployed position. In contrast, the Mars-fixed (M) coordinate system used for rover navigation has X north, Y east, and Z down, with its origin at the center of the base of the lander. We believe that the "Z-up" LSC system will significantly reduce confusion for future users of planimetric maps. Our hard copy maps include a primary LSC grid and supplementary tick marks for M-frame coordinates; simple software for conversion between the two systems are archived with digital products.

Level 3 processing generally involves photometric correction to remove brightness variations from scene to scene which are primarily due to illumination differences. This step currently is not implemented for IMP data processing. Prior to the mission, there were no plans to obtain and return images within a sequence at widely varying times of day. The Super Pan sequence incorporates such widely varying local times in a single panorama, both by intent (to optimize illumination in different parts of the site) and to meet constraints on data acquisition and return. Photometric modeling and Level 3 processing of the Super Pan is therefore needed in order to generate products of the highest cosmetic quality. To date, such cosmetic tone-matching of the Super Pan images for hard copy purposes has been carried out entirely interactively. Tests suggest, however, that a very simple photometric correction (a gain factor calculated for each image based on a quadratic fit to the measured intensity of soil patches versus time of day) can reduce the cube-to-cube brightness variations by a factor of ~4. To facilitate possible future updates, this correction is designed to be reversible via use of a multiplicative factor (for each filter) calculated for a horizontal surface. Photometric modeling (though not correction) has been carried out because of its scientific interest [Johnson *et al.*, this issue].

The final, or Level 4, processing of IMP images involves creation of a multispectral mosaic from individual cubes. Although manual adjustment and positioning of single-band image frames was required to support mission and science activities shortly after IMP data were acquired, with the more recent establishment of geometric control, the production of 7-, 8-, and 15-band multispectral mosaics has been conducted via automatic adjustment of cubes (using the ISIS program RECMOS). Depending on the target audience, this step may be followed by efforts to enhance presentation of the resulting mosaics, including cosmetic filtration, frame-to-frame brightness matching to remove seams, addition of grids or other annotation, and color enhancement or anaglyphic presentation.

Plate 2. IMP mosaics displayed as anaglyphic stereo images (filter 5 (0.67 μm =red), left and right eye views). (top) An uncontrolled mosaic of 10 Super Pan images produced with the original command pointing (note offsets at image frame boundaries); (middle) A semicontrolled mosaic made by manually adjusting the relative positions of the images (note that the offsets are reduced substantially, but a gap has been exposed); and (bottom) A controlled mosaic derived by bundle adjustment of camera pointing and ground control point coordinates (the gap is filled with a single Monster Pan image).



ISIS also has software tools to support a variety of advanced processing tasks for IMP data analysis. These science tasks include (but are not limited to) modeling of the surface photometric function to characterize surface textures and shapes, photoclinometric or “shape-from-shading” analyses of IMP data and derived DTMs (both described by Kirk *et al.* [this issue]), use of coregistered image sequences from different panoramas to detect and visualize changes in the scenes with time, and synthesis of full color stereo views incorporating either real color and synthetic stereo data (as in the case of rectification to a “third eye” or hypothetical vantage point such as the center of the IMP camera head) or real stereo and synthetic color images (using the ISIS program BNDYNPRC to synthesize “missing” data based on statistical analysis of adjacent images in a cube).

5. Cartographic Products of the MPF Mission

IMP cartographic products in the USGS archive include spectral cubes, panoramic maps, planimetric maps, and topographic and ancillary data (Table 3). As noted above, products are classified most broadly by the type of data they contain (images or geometric information) and their coordinate system: point-perspective as per the input images; panoramic or azimuthal coverage; and planimetric (i.e., in Cartesian “top” view). The image products may be thought of as spectral image “cubes,” having in addition to the usual line and sample coordinates a third (band or spectral) dimension. The ISIS system can be used to manipulate such cubes regardless of the number of bands; transparent handling of multispectral image cubes is the most fundamental design principle of ISIS. To make the data more accessible to users with other software systems that may lack this multiband image capability, the image sets are broken into multiple files for archiving, one for each spectral band. These sets of files may readily be ingested and reassembled into a multiband format, and we continue to refer to each set of corresponding image files as a cube in this paper. To minimize degradation of spectral data by reprojection, stereo-coregistered sets of 15-filter images from the Super Pan are archived both with original geometry and with a point-perspective geometry intermediate between the left and right cameras. Panoramic mosaics made from all five major image sets are archived in Macauley-Kirk projection, and the Super Pan 15-band coregistered data are mosaicked in cylindrical projection. Only a representative subset of the images are archived in planimetric form. The topographic data sets may themselves be divided into point-perspective, panoramic, and planimetric formats, coregistered to the image products and intended to be used in conjunction with them. Additional or ancillary data, produced as a natural outcome of data processing, include (1) improved camera pointing data for each processed image, (2) shifts in relative lander position and orientation, (3) a table of features used in the establishment of a ground control system, and (4) a table of the match points used to establish range information between image pairs derived from stereogrammetric processing.

5.1. Spectral Cubes

Of the 144 positions in the Super Pan sequence, 119 (23 half-height and 96 full-height) positions had data for all 15 filters returned. Each full-height position is 248 lines by 256

Table 4. IMP Point-Perspective Image Products

Product	Size, Mbytes	Bands	Filters-Eye
SCL 1 - 119	120	8	0-5-6-7-8-9-10-11-L
SCR 1 - 119	105	7	0-5-6-8-9-10-11-R
SCLR 1 - 119	105	15	All filters, both eyes (rectified/coregistered)
Total	450		

samples by 15 bands with 2 bytes per pixel. For each position, three spectral cube products (Table 4) have been generated: (1) eight-band registered right camera, (2) seven-band registered left camera, and (3) 15-band consisting of left and right camera data rectified to a common position intermediate between the two cameras. These 357 (119 x 3) cubes will allow for a variety of spectral processing and analysis tasks.

5.2. Panoramic Maps

All five major cartographic data sets are mosaicked and archived in panoramic format, including all spectral bands. Left and right camera data are included in separate mosaics in Macauley-Kirk projection, but the Super Pan data also have been rectified (to coregister the images from the two cameras) and compiled into a 15-band mosaic in cylindrical projection. The maximum size of an IMP panorama, for full azimuth and elevation coverage, is approximately 6000 samples by 900 to 1400 lines (depending on the data set and type of projection) with the possibility of one or more bands. Each pixel in a band is 16-bit data and requires two bytes; therefore data storage requirements are 12 to 17 Mbytes per band. Included with each pan will be an image at 1/4-resolution that indicates the image used for each location in the mosaic. These index mosaics contribute negligibly to the data volume, requiring ≤ 0.5 Mbyte each at 8 bits per pixel. Table 5 shows the planned panoramic map products for IMP. Note that Pans 1 and 3 have only 50% of the azimuth range and so require half the storage per band. Also, Pan 11 contains all 15 bands, with seven right eye bands geometrically merged to the eight left eye bands.

We also plan to archive another panoramic data set, not included in Table 5. Parker [1998] and Kanefsky *et al.* [1998] have demonstrated that the spectral bands of the Super Pan can be combined by sharpening, interactive coregistration, and averaging to yield a product with “superresolution” in which features smaller than an IMP pixel are resolved. This process is a simple alternative to the more rigorous approach to superresolution described by Stoker *et al.* [this issue], which has not been successfully applied to the multispectral Super Pan data. Parker’s process yields images with the geometric properties of an IMP frame, but enlarged, typically by a factor of 5 linearly. The original-resolution color data may be merged with the superresolved frame; for the left camera it is necessary to synthesize a green band as a linear combination of red and blue. The color superresolved images are reprojected and mosaicked in ISIS, then processed interactively with Adobe Photoshop to yield the optimum cosmetic quality in terms of color balance and seam feathering. The gaps in the Super Pan are filled with nonsuperresolved data. The resulting data set consists of 2

Table 5. IMP Panoramic Image Products

Product	Sequence	Size, Mbytes	Bands	Filters-Eye
Pan 1	First Look	6.4	1	5-L
Pan 2	First Look	12.8	1	5R
Pan 3	First Look	19.2	3	0-5-9-R
Pan 4	Insurance	12.8	1	0-L
Pan 5	Insurance	51.2	4	0-6-8-9-R
Pan 6	Monster	17.2	1	5-L
Pan 7	Monster	51.6	3	0-5-9-R
Pan 8	Gallery	51.6	3	0-5-9-R
Pan 9	Super	137.6	8	0-5-6-7-8-9-10-11-L
Pan 10	Super	129.4	7	0-5-6-8-9-10-11-R
Pan 11*	Super	198.0	15	all L and all R
Total		687.8		

* Rectified, in cylindrical projection; all others in Macauley-Kirk projection.

three-band panoramas, one from each camera, of ~30,000 samples and ~7000 lines, which are divided into smaller tiles. Because this data set is intended mainly to support qualitative morphologic and color studies, 8 bits per band and lossy compression are deemed acceptable for archiving. Tests show that Joint Photographic Experts Group (JPEG) compression at 10:1 introduces only one to two data numbers of RMS error. The total volume of the superresolved data set with such compression is ~130 Mbytes.

5.3. Planimetric Maps

The complete set of sequences and filters is mosaicked and archived only in panoramic form. Planimetric maps, which are of interest mainly for spatial/morphological investigations, with "natural" color to discriminate features, are produced only for a representative subset of the data. The primary goal is to produce two planimetric maps which preserve the highest resolution of the data nearest to the lander (approximately 1 mm/pixel at predeploy (Insurance Pan) and 2 mm/pixel postdeploy (Gallery Pan)). A third map based on Gallery Pan data extends farther from the lander but at reduced resolution. The maps have three bands each with two bytes per pixel. CD-ROM storage capacity limits the planimetric maps to a practical maximum of 10,000 lines and samples, which leads to 575 Mbytes (10,000x10,000x3x2) per map. Because of their size, each map is tiled and reduced ("browse" versions will be included, though these will not increase the total data volume significantly). Table 6 lists IMP planimetric map products. Note that Plan 3 may be changed to 8 mm/pixel, which would extend to 40 m if the appearance is satisfactory. The planimetric maps are orthorectified using detailed topographic information produced in SOCET Set.

Table 6. IMP Planimetric Image Products

Product	Sequence	Size, Mbytes	Filters- Eye	Resolution- Distance
Plan 1	Insurance	600	0-6-9-R	1 mm to 5 m
Plan 2	Gallery	600	0-5-9-R	2 mm to 10 m
Plan 3	Gallery	600	0-5-9-R	4 mm to 20 m
Total		1800		

5.4. Topographic Data

There are three groups of topographic products in the USGS IMP data archive (Tables 7, 8, 9). The first group (Table 7) of topographic products consists of three sets of 119 individual spectral cubes, each with six bands total: three bands of positional information (representing the x, y, and z positions at each pixel) and three bands of local surface normals (each band is in 16-bit format and requires 2 bytes per pixel). To achieve the required dynamic range with 16 bits, the X and Y coordinates are stored as the signed square root of the actual value. The second group of products (Table 8) consists of geometric data that have been generated for mosaics in predeploy and postdeploy right and left eye geometry (Macauley-Kirk projection) and synthesized post-deploy "third-eye" geometry (in cylindrical projection), corresponding to the various panoramas in Table 5. The third group of topographic products (Table 9) consists of two planimetric DTMs. The DTMs are 5000 samples by 5000 lines with 16-bit Z-value (elevation) pixel representations only.

To summarize, four CD-ROM volumes containing IMP cartographic data products have been produced by the USGS (assuming that each CD-ROM contains ~650 Mbytes of data and that lossless compression of the data will save about 1/3 of the total volume).

6. Science Applications of MPF Cartographic Products

A variety of science tasks can be accomplished with IMP cartographic products and their derivatives. The color planimetric and panoramic maps and mosaics have been used extensively to support geologic characterization of the landing

Table 7. IMP Spectral Cube Products

Product	Size, Mbytes	Registers to Image Number
Topo SCL 1 - 119	76	SCL 1 - 119
Topo SCR 1 - 119	76	SCR 1 - 119
Topo SCLR 1 - 119	76	SCLR 1 - 119
Total	228	

Table 8. IMP Topographic Data Products: Panoramic DTMs

Product	Size, Mbytes	Registers to Pan Number
Topo Pan 1	77	1, 4
Topo Pan 2	77	2, 3, 5
Topo Pan 3	103	6, 9
Topo Pan 4	103	7, 8, 10
Topo Pan 5	80	11
Total	440	

site, including geomorphologic studies of the site topography, landforms, and features [Golombek *et al.*, 1997b]. Determinations of the topography of the MPF landing site and environs out to ~60 m [Kirk *et al.*, this issue; Ward *et al.*, this issue] have assisted in unraveling the history of the large- and small-scale geologic processes (such as fluvial and mass flow episodes and eolian deposition and deflation events) which have shaped the observed MPF landing site. Analyses of the distribution, surface characteristics, and reflectance spectra of soils and rocks [e.g., Bell *et al.*, 1997, 1998; Britt *et al.*, 1997, 1998; McSween *et al.*, this issue; Smith *et al.*, 1997a; Murchie *et al.*, 1997, 1998] have been extended by spectroscopic analyses of surface materials (rocks, soils, drift materials, etc.) conducted using coregistered, multispectral IMP Super Pan mosaics [e.g., Bell *et al.*, 1997, 1998; Britt *et al.*, 1997, 1998; Bridges *et al.*, 1998]. Versions of these products were radiometrically calibrated to relative reflectance (R^* , measured relative to an on board calibration target observed at the same time of day) using version 1.0 of the IMP calibration algorithm of Reid *et al.* [1997, this issue]. Spectra at 8 (left eye) and 7 (right eye) wavelengths were extracted and combined to evaluate the mineralogy of Martian surface materials, in conjunction with results from the magnetic properties experiment [Hviid *et al.*, 1997] and chemical analyses from the alpha X ray proton spectrometer (APXS [Reider *et al.*, 1997b]). These spectrally calibrated image mosaics are estimated to be accurate to within 10 to 15% absolute and 2 to 4% relative reflectance in most cases [Smith *et al.*, 1997a; Reid *et al.*, 1997]. Derived products from the multispectral mosaics (Figure 2) include, for example, thematic maps of spectral units such as those depicted in the red/blue ratio images (0.67/0.44 μm ; this is similar to the slope parameter of Guinness *et al.* [1987] and is used as a measure of oxidation state of iron-bearing minerals) and the spectral curvature maps (this ratio of red/green (0.67/0.53 μm) and green/blue (0.53/0.44 μm) ratios depicts the ferric absorption edge and is thought to be related to ferric oxide mineral type and degree of crystallinity [e.g., Guinness *et al.*, 1987; Bell *et al.*, 1997, 1998]).

Sources of uncertainty in the absolute spectral calibration of the IMP mosaics include photometric variability of the calibration targets [Arnold *et al.*, 1997; Reid *et al.*, 1997] and the influence of strongly colored diffuse sky illumination on the scene [Keller *et al.*, 1997; Wuttke *et al.*, 1997; Maki *et al.*, this issue; Thomas *et al.*, this issue]. Some efforts to characterize and to resolve these difficulties have also relied upon multispectral image mosaics produced from IMP data in conjunction with data collected by IMP for the same targets under differing illumination conditions [e.g., Johnson *et al.*, 1997, 1998]. These photometric and spectral data are used to characterize surface roughness, particle size distributions, and

surface coatings of materials at the MPF landing site [Johnson *et al.*, this issue]. Sophisticated analyses of shapes and slopes in IMP mosaics are made possible by the variation of times-of-day of imaging and thus illumination intensity and direction in the IMP data. For example, in combination with a model of the diffuse illumination and a surface photometric function, local surface-normal (spatial orientation) data for scene elements in the IMP mosaics can be used to provide information on shape and textures of surface materials, and thus to permit detailed analyses of the nature and origins of observed landforms and features.

7. Summary

The USGS IMP cartographic products described here represent one major element of the MPF data archive (other elements are described by Kirk *et al.* [this issue] and LaVoie *et al.* [this issue]) and will provide a valuable resource for science analyses of the surface of Mars as observed at Ares Vallis. The USGS IMP data archive represents a substantial amount of effort, largely in the form of specialized software development to accommodate and take advantage of the characteristics of the IMP camera and its data. In part because of these unique characteristics but also because of the much larger than anticipated issue of returned data, the size and complexity of the task of data processing for the panoramic/close-range stereo IMP camera system were underestimated. Planning for future landed camera missions should include realistic extremes of mission duration and data rate to avoid the need for on-the-fly rescoping and the resulting inefficiencies in data collection; during the excitement of the active mission, attention is diverted from the details of imaging sequence design. Similar advice can be directed to the development of a cartographic processing plan; an accurate and complete plan, with budgets developed for different imaging and data rate scenarios, requires advanced planning and coordination with data collection during the active mission.

The Super Pan imaging sequence incorporated widely varying local times in a single panorama, both intentionally (to optimize illumination in different parts of the site) and to meet constraints on data acquisition and return. In future landed camera missions where data return constraints make it feasible, multispectral data acquisition for any given region could be scheduled at consistent times of day or even multiple times of day to facilitate complete characterization of the shapes and spectroscopic signatures of surface materials.

The design and use of paired filters for three of the IMP filter-wheel locations have been validated by use of these data for stereo matching. The detailed DTMs derived from the IMP stereo filters have facilitated matching and coregistration of all spectral bands into several 15-filter multispectral data sets. However, the reduced contrast between the 0.67 μm (R) and 0.965 μm (IR) stereo filters, and the resulting difficulty

Table 9. IMP Topographic Data Products: Planimetric DTMs

Product	Size, Mbytes	Resolution-Distance
Topo Plan 1	50	4 mm to 10 m
Topo Plan 2	50	32 mm to 80 m
Total	100	

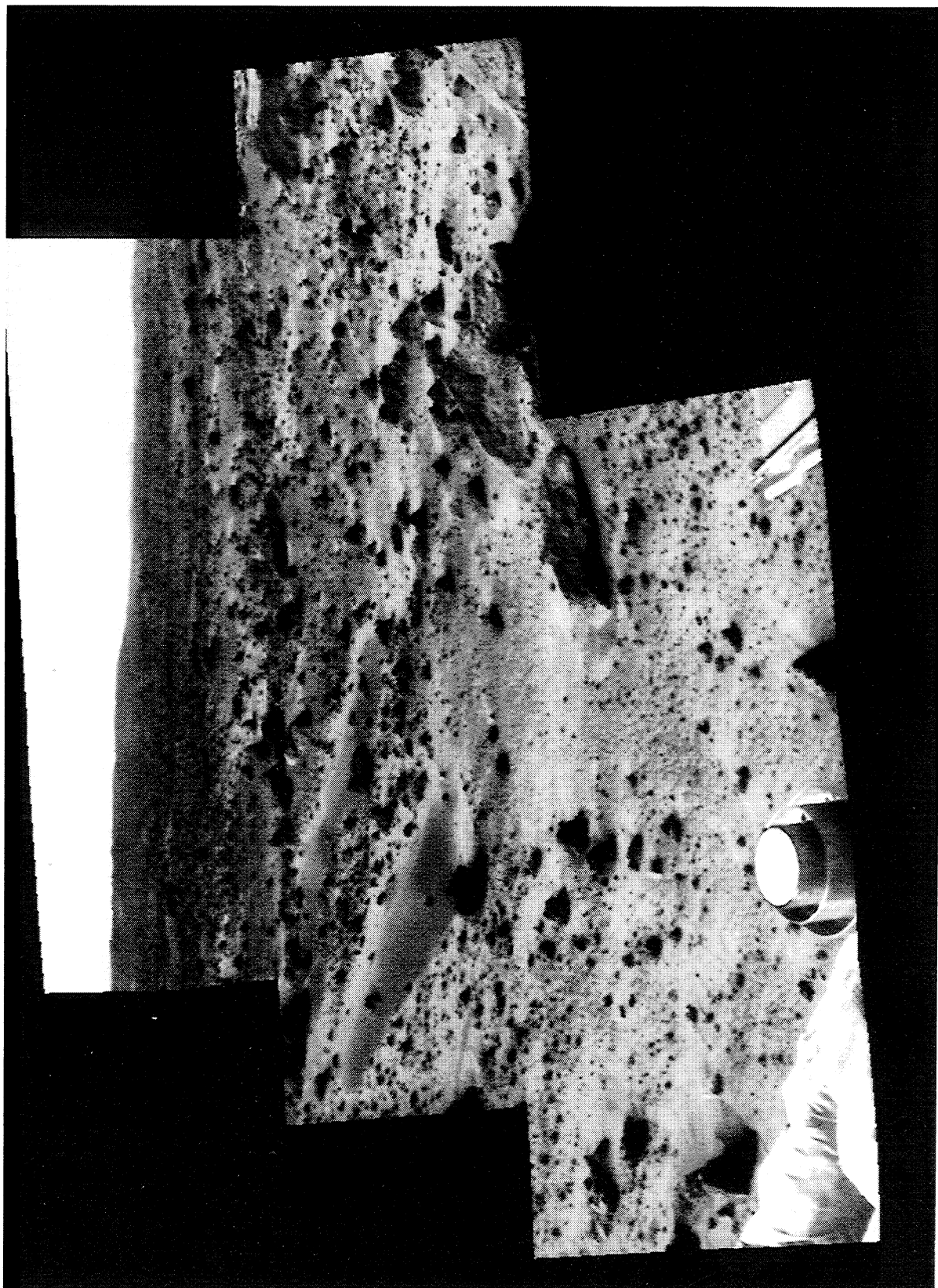


Figure 2a. Example of a spectral unit map derived from multispectral IMP mosaics of the Mermaid dune form area of the Super Pan: right eye view obtained at 0.67 μm . Mermaid dune form is in the left center of the view, the rocks Hassock and Ender are seen in the right center, and Far Knob is faintly seen on the horizon just right of center (compare with Plate 6 of *Smith et al.* [1997a]). Note that Mermaid and other dune forms are moderately dark ("dark soil" of *Smith et al.* [1997a]), soils are lighter, fine ("drift") materials are lightest, and the rocks are moderately dark with shadows.

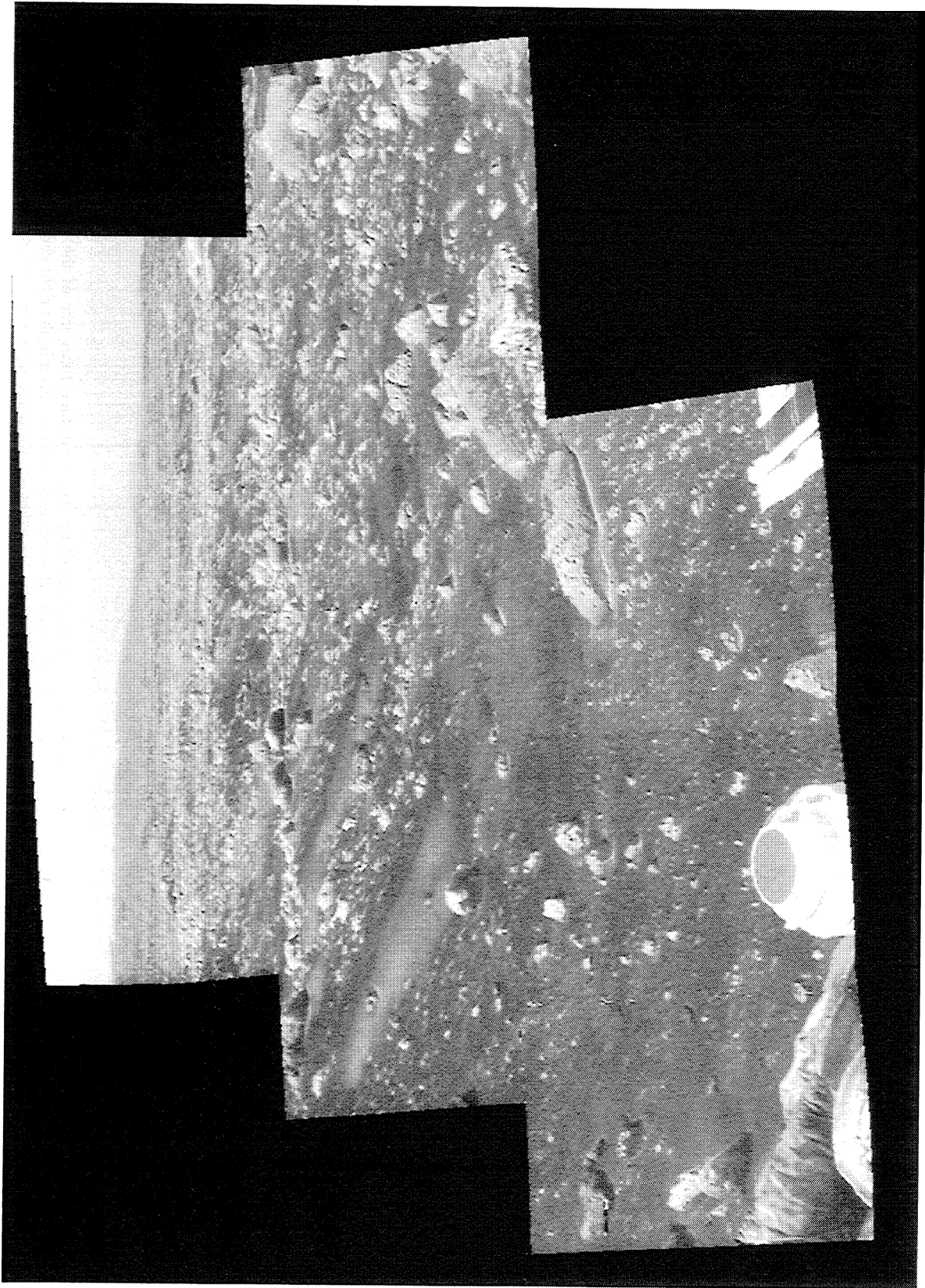


Figure 2b. Map of the "curvature index" parameter [e.g. Guinness *et al.*, 1987], which can be thought of as the ratio of the right eye filters (red/green) to (green/blue), or (0.67/0.53 μm) to (0.53/0.44 μm). In this map, shadows are subdued, rock surface textures are enhanced, and dune forms are relatively bright (Mermaid dune form may have larger particle sizes than most other soil materials, or it may have an intermediate degree of ferric iron crystallinity such as might be expected for a locally derived, weathered soil).

with automated stereo matching and DTM extraction, leads us to note that the inclusion (as a substitution for IR?) of a green-filter stereo image pair (~0.55 μm wavelength) would be most useful for obtaining "true color stereo" views as well as for photogrammetric and geometric processing.

Finally, the software tools and capabilities utilized in these cartographic efforts are now in place; many of them are already in the public domain. Much of this development work, including the operational experience gained by the cartographic processing team, will apply to data returned by landed cameras planned for future planetary missions.

Acknowledgments. We are grateful for review comments from W. Calvin, H. Kieffer, D. Hirsch (USGS), and two anonymous reviewers. We congratulate and thank the Mars Pathfinder scientists and engineers responsible for successfully landing and operating on Mars in 1997.

References

- Arnold, G., A. Dummel, H. Nordmeyer, P. Smith, and D. Britt, Laboratory reflectance measurements of ferric oxides, phyllosilicates and palagonitic soils as Mars analog materials and study of the calibration targets of the Imager for Mars Pathfinder (IMP) (abstract), *Eos, Trans. AGU, 78*, Fall Meet. Suppl., F403, 1997.
- Batson, R.M., Cartography, in *Planetary Mapping*, edited by R. Greeley and R.M. Batson, pp. 60-95, Cambridge Univ. Press, New York, 1990.
- Bell, J.F., III, et al., Mineralogy and diversity of soils at the Mars Pathfinder landing site (abstract), *Eos, Trans. AGU, 78*, Fall Meet. Suppl., F396, 1997.
- Bell, J.F., III, et al., 1998, Mineralogy, composition, and origin of soil and dust at the Mars Pathfinder landing site (abstract), *Lunar Planet. Sci. XXIX*, 1723-1724, 1998.
- Bridges, N.T., J.F. Bell III, J. Crisp, T. Economou, J.R. Johnson, S.L. Murchie, and R.J. Reid, Comparison between APXS and IMP multispectral data at the Pathfinder landing site: Evidence for dust coatings on rock surfaces (abstract), *Lunar Planet. Sci. XXIX*, 1534-1535, 1998.
- Bridges, N.T., R. Greeley, A.F.C. Haldeman, K.E. Herkenhoff, M. Kraft, T.J. Parker, and A.W. Ward Jr., Ventifacts at the Pathfinder landing site, *J. Geophys. Res.*, this issue.
- Britt, D.T., et al., The mineralogy of the Mars Pathfinder landing site (abstract), *Eos, Trans. AGU, 78*, Fall Meet. Suppl., F395, 1997.
- Britt, D.T., et al., The mineralogy of the Mars Pathfinder landing site (abstract), *Lunar Planet. Sci. XXIX*, 1776-1777, 1998.
- Crowe, D.G., et al., *Imager for Mars Pathfinder Calibration Report*, version 10, Lunar and Planet. Lab., Univ. of Ariz., Tuscon, Sept. 30, 1996.
- Eliason, E.M., Production of digital image models (DIMs) (abstract), *Lunar and Planet. Sci., XVIII*, 331-332, 1997.
- Gaddis, L.R., et al., An overview of the Integrated Software for Imaging Spectrometers (ISIS) (abstract), *Lunar Planet. Sci., XVIII*, 387-388, 1997.
- Gaddis, L., et al., The Mars Pathfinder "Super Pan": A USGS cartographic product (abstract), *Lunar Planet. Sci. XXIX*, 1831-1832, 1998.
- Golombek, M.P., The Mars Pathfinder mission, *J. Geophys. Res.*, 102, 3953-3965, 1997.
- Golombek, M.P., R.A. Cook, H.J. Moore, and T.J. Parker, Selection of the Mars Pathfinder landing site, *J. Geophys. Res.*, 102, 3967-3988, 1997a.
- Golombek, M.P., et al., Assessment of landing site predictions, *Science*, 278, 1743-1748, 1997b.
- Guinness, E.A., R.E. Arvidson, M.A. Dale-Bannister, R.B. Singer, and E.A. Bruckenthal, On the spectral reflectance properties of materials exposed at the Viking landing sites, *Proc. Lunar Planet. Sci. Conf. 17th, part 2*, *J. Geophys. Res.*, 92, suppl., E575-E587, 1987.
- Hviid, S.F., et al., Magnetic properties experiments on the Mars Pathfinder lander: Preliminary results, *Science*, 278, 1768-1770, 1997.
- Johnson, J.R., et al., Preliminary photometric analysis of selected materials at the Sagan Memorial Station, Mars (abstract), *Eos, Trans. AGU, 78*, Fall Meet. Suppl., F402, 1997.
- Johnson, J.R., et al., Photometric imaging sequences and analysis at the Mars Pathfinder landing site (abstract), *Lunar Planet. Sci. XXIX*, 1228-1229, 1998.
- Johnson, J.R., et al., Preliminary results on photometric properties of materials at the Sagan Memorial Station landing site, Mars, *J. Geophys. Res.*, this issue.
- Kanefsky, B., T.J. Parker, and P.C. Cheeseman, 1998, Super-resolution results from Pathfinder IMP (abstract), *Lunar Planet. Sci. XXIX*, 1536-1537, 1998.
- Keller, U., W.J. Markiewicz, N. Thomas, M.W. Wuttke, R. Sablotny, and P.H. Smith, Effects of atmospheric aerosols on colour of geologic materials - Imager for Mars Pathfinder (abstract), *Eos, Trans. AGU, 78*, Fall Meet. Suppl., F395, 1997.
- Kirk, R.L., E. Howington-Kraus, T. Hare, and E. Dorner, Cartography of the Mars Pathfinder landing site (abstract), *Eos, Trans. AGU, 78*, Fall Meet. Suppl., F404, 1997.
- Kirk, R.L., et al., Mapping the Sagan Memorial Station site with the IMP camera (abstract), *Lunar Planet. Sci. XXIX*, 1752-1753, 1998.
- Kirk, R.L., et al., Digital photogrammetric analysis of the IMP camera images: Mapping the Mars Pathfinder landing site in three dimensions, *J. Geophys. Res.*, this issue.
- LaVoie, S.K., et al., Processing and analysis of Mars Pathfinder science data at the Jet Propulsion Laboratory's Science Data Processing Systems Section, *J. Geophys. Res.*, this issue.
- Maki, J.N., J.J. Lorre, P.H. Smith, R.D. Brandt, and D.J. Steinwand, The color of Mars: Spectrophotometric measurements at the Pathfinder landing site, *J. Geophys. Res.*, this issue.
- McSween, H.Y., Jr., et al., Chemical, multispectral, and textural constraints on the composition and origin of rocks at the Mars Pathfinder landing site, *J. Geophys. Res.*, this issue.
- Murchie, S., et al., Spectral properties and classes of rocks at the Mars Pathfinder landing site (abstract), *Eos, Trans. AGU, 78*, Fall Meet. Suppl., F396, 1997.
- Murchie, S., J. Johnson, H. McSween, N. Bridges, R. Anderson, D. Britt, J.F. Bell, III, and J. Crisp, Spectral properties of rocks at the Mars Pathfinder landing site (abstract), *Lunar Planet. Sci. XXIX*, 1444-1445, 1998.
- Parker, T.J., "Superresolution" of the Mars Pathfinder landing site using manual techniques (abstract), *Lunar Planet. Sci. XXIX*, 1817-1818, 1998.
- Reid, R.J., A. Dummel, R.B. Singer, J.R. Johnson, J.F. Bell III, and T. Daley, Imager for Mars Pathfinder calibration (abstract), *Eos, Trans. AGU, 78*, Fall Meet. Suppl., F402, 1997.
- Reid, B., et al., IMP image calibration, *J. Geophys. Res.*, this issue.
- Rieder, R., H. Wanke, T. Economou, and A. Turkevich, Determination of the chemical composition of Martian soil and rocks: The alpha proton X ray spectrometer, *J. Geophys. Res.*, 102, 4027-4044, 1997a.
- Rieder, R., T. Economou, H. Wanke, A. Turkevich, J. Crisp, J. Bruckner, G. Dreibus, and H.Y. McSween Jr., The chemical composition of martian soil and rocks returned by the mobile alpha proton X ray spectrometer: Preliminary results from the X-ray mode, *Science*, 278, 1771-1774, 1997b.
- Rover Team, The Pathfinder microrover, *J. Geophys. Res.*, 102, 3989-4001, 1997a.
- Rover Team, Characterization of the martian surface deposits by the Mars Pathfinder rover, Sojourner, *Science*, 278, 1765-1768, 1997b.
- Schofield, J.T., J.R. Barnes, D. Crisp, R.M. Haberle, S. Larsen, J.A. Magalhães, J.R. Murphy, A. Seiff, and G. Wilson, The Mars Pathfinder atmospheric structure investigation/meteorology (ASI/MET) experiment, *Science*, 278, 1752-1758, 1997.
- Seiff, A., et al., The atmosphere structure and meteorology instrument on the Mars Pathfinder lander, *J. Geophys. Res.*, 102, 4045-4056, 1997.
- Smith, P.H., et al., Results from the Mars Pathfinder camera, *Science*, 278, 1758-1764, 1997a.
- Smith, P.H., et al., The imager for Mars Pathfinder experiment, *J. Geophys. Res.*, 102, 4003-4025, 1997b.
- Soderblom, L.A., et al., The Mars Pathfinder Super Pan: U.S. Geological Survey processing and analysis (abstract), *Eos, Trans. AGU, 78*, Fall Meet. Suppl., F404, 1997.

- Stoker, C., T. Blackmon, J. Hagan, B. Kanefsky, C. Neveu, K. Schwehr, M. Simms, and E. Zbinden, MarsMap: Analyzing Pathfinder data using virtual reality (abstract), *Eos, Trans. AGU*, 78, Fall Meet. Suppl., F403, 1997.
- Stoker, C.R., E. Zbinden, T.T. Blackmon, B. Kanefsky, J. Hagen, C. Neveu, D. Rasmussen, K. Schwehr, and M. Sims, Analyzing Pathfinder data using virtual reality and superresolved imaging, *J. Geophys. Res.*, this issue.
- Thomas, N., W.J. Markiewicz, R. Sablotny, M.W. Wuttke, H.U. Keller, and P.H. Smith, The color of the Martian sky and its influence on the illumination of the Martian surface, *J. Geophys. Res.*, this issue.
- Torson, J., and K. Becker, ISIS---A software architecture for processing planetary images (abstract), *Lunar Planet. Sci. XVIII*, 1443-1444, 1997.
- Ward, A.W., L.R. Gaddis, R.L. Kirk, L.A. Soderblom, K.L. Tanaka, M.P. Golombek, T.J. Parker, R. Greeley, and R.O. Kuzmin, General geology and geomorphology of the Mars Pathfinder landing site, *J. Geophys. Res.*, this issue.
- Wuttke, M.W., N. Thomas, H.U. Keller, P.H. Smith, C. Stoker, and T. Blackmon, Monte Carlo modeling of the diffuse flux near rocks (abstract), *Eos, Trans. AGU*, 78, Fall Meet. Suppl., F402, 1997.
-
- J. Barrett, K. Becker, T. Becker, J. Blue, D. Cook, E. Eliason, L.R. Gaddis, T. Hare, E. Howington-Kraus, C. Isbell, J.R. Johnson, R.L. Kirk, E.M. Lee, B. Redding, L.A. Soderblom, R. Sucharski, T. Sucharski, and A. W. Ward, Astrogeology Program, U.S. Geological Survey, 2255 North Gemini Drive, Flagstaff, AZ 86001. (lgaddis@flagmail.wr.usgs.gov)
D.T. Britt and P. Smith, Lunar and Planetary Laboratory, University of Arizona, 1629 East University Boulevard, Tucson, AZ 85721.

(Received February 26, 1998; revised September 10, 1998; accepted September 15, 1998.)